European Journal of
Nuclear
Medicine

Original article

Specific targeting of infectious foci with radioiodinated human recombinant interleukin-1 in an experimental model

Conny J. van der Laken[1], Otto C. Boerman[1], Wim J.G. Oyen[1], Marjo T.P. van de Ven[1], Roland A.M.J. Claessens[1], Jos W.M. van der Meer[2], Frans H.M. Corstens[1]

[1] Department of Nuclear Medicine, University Hospital Nijmegen, Nijmegen, The Netherlands
[2] Department of Internal Medicine, University Hospital Nijmegen, Nijmegen, The Netherlands

Received 1 May and in revised form 8 June 1995

Abstract. In the present study, radioiodinated human recombinant interleukin-1 (IL-1) was investigated for its potential to image infectious foci in vivo in an animal model of infection. Twenty-four hours after induction of a *Staphylococcus aureus* abscess in the left calf muscle, mice were i.v. injected with both iodine-125 labelled IL-1 and iodine-131 labelled myoglobin, a size-matched control agent. The animals were killed for tissue biodistribution studies at 2, 6, 12, 24 and 48 h p.i. Gamma camera images were obtained at 6, 24 and 48 h after injecting mice with ^{123}I-IL-1. Radioiodinated IL-1 rapidly cleared from the body; after 12 h the abscess was the organ with the highest activity. The absolute abscess uptake of ^{125}I-IL-1 remained high compared to ^{131}I-myoglobin, resulting in significantly higher abscess-to-muscle ratios of ^{125}I-IL-1 compared to ^{131}I-myoglobin. The ratios of ^{125}I-IL-1 reached the ultimate value of 44.4±10.8 at 48 h p.i., whereas the ratios of ^{131}I-myoglobin did not exceed 5.9±0.7. Gamma camera imaging revealed clearly visible abscesses. In conclusion, our results demonstrate specific retention of radioiodinated IL-1 in the abscess, presumably by interaction of IL-1 with its receptor on the inflammatory cells. The high target-to-background ratios that were obtained over the course of time indicate that the IL-1 receptor may be a valuable target for the imaging of infectious foci.

Key words: Radioiodination – Interleukin-1 – Infection – Biodistribution – Radionuclide imaging

Eur J Nucl Med (1995) 22:1249–1255

Correspondence to: C.J. van der Laken, Department of Nuclear Medicine, University Hospital Nijmegen, P.O. Box 9101, 6500 HB Nijmegen, The Netherlands

Introduction

Adequate localization of active infectious and inflammatory lesions contributes to elucidation of the cause of the disease and introduction of the appropriate therapy. However, each of the currently used radiological or scintigraphic techniques for detection of infectious foci has limitations. In the early phase of infection, when there are no substantial anatomical changes, radiological techniques including computerized tomography and ultrasonography will not reveal any abnormality. Conventional scintigraphic techniques, such as IgG scintigraphy and gallium scintigraphy can provide the information in such situations but these techniques require at least 24 h to establish a definitive diagnosis [1].

The ideal radiopharmaceutical for scintigraphic detection of focal sites of infection should yield a same-day answer in order to meet the needs of clinical practice. It should therefore show high and rapid accumulation in the abscess, fast blood clearance and low physiological organ uptake [2]. The development of an imaging technique which uses a small molecule able to bind specific receptors in the infectious focus is therefore desirable. A possibility could be the use of cytokines. Two studies have recently shown that cytokines are indeed potential agents to image infectious foci. Firstly, Signore et al. showed that iodine-123 labelled IL-2 can be used to visualize pancreatic lymphocytic infiltration in non-obese diabetic mice [3]. Secondly, Hay et al. reported that radioiodinated IL-8 had a better performance than either gallium-67 citrate or indium-111 labelled leucocytes in the detection of acute inflammatory lesions in a rat model [4].

In this study the potential of another radioiodinated cytokine, human recombinant interleukin-1, was explored. Interleukin-1 (IL-1) is a 17-kDa protein mainly produced by mononuclear phagocytes in response to an inflammatory stimulus. Two forms of IL-1 (IL–1α and IL-1β) have been identified. Although both forms are

distinct gene products, they recognize the same cell surface receptors and share various biological activities. Recent studies have shown that two major IL-1 receptor (IL-1R) molecules can be distinguished. On T cells, fibroblasts, endothelial cells and hepatocytes, an 80-kDa IL-1R (type I) is consistently observed whereas neutrophils, monocytes and B cells express a 68-kDa IL-1R (type II). The binding affinity of IL-1 for the IL-1R is in the picomolar range ($K_a = 10^9$–10^{11} M^{-1}), depending on the receptor type and IL-1 form [5].

Infection and inflammation are characterized by an influx of leucocytes [6], being predominantly IL-1R positive cells. Because of the high affinity for its receptor, IL-1 might be able to specifically target to these inflammatory cells. The specific receptor binding may lead to a greater specificity for imaging inflammatory conditions. In addition, IL-1 rapidly clears from the blood; following intravenous (i.v.) administration in mice, IL-1 showed an initial half-life of 5–10 min [7]. Because of these favourable physicochemical characteristics, scintigraphy with IL-1 may be a useful technique for early and specific localization of infectious foci. In the present study, we investigated whether radioiodinated IL-1 can be used to visualize infectious foci in an animal model of infection.

Materials and methods

Radiolabelling of IL-1

Human recombinant IL-1α (IL-1) (specific activity of 3×10^8 U/mg), kindly provided by Dr. P. Lomedico (Hoffman-La Roche, Nutley, N.J.), was radiolabelled using the iodogen method [8]. Briefly, 3 µg IL-1 (0.68 mg/ml) in 15 µl 0.5 *M* and 70 µl 50 m*M* phosphate buffer, pH 7.2 and 37 MBq $Na^{125}I$ (Amersham International, Amersham, UK; specific activity of 570 GBq/mg) were added to glass tubes, precoated with 1,3,4,6-tetrachloro-3α,6α-diphenylglucouril (Pierce, Rockford, Ill.) (25 µg/100 µl). The reaction was allowed to proceed for 10 min at room temperature, after which the reaction mixture was eluted with 0.5% BSA in PBS on a Sephadex G-25 column (PD-10; Pharmacia, Uppsala, Sweden) to separate labelled IL-1 from free ^{125}I. The void fractions were pooled and sterilized through a 0.2-µm filter.

Analogously, 3 µg myoglobin (Sigma, St. Louis, Mo.) (1 mg/ml), a protein with a similar molecular weight (18 kDa) to IL-1 without any known interactions in vivo, was labelled with $Na^{131}I$ (Medgenix, Fleurus, Belgium; specific activity of >185 GBq/mg). Myoglobin served as the non-specific control agent in the biodistribution experiments.

For the purpose of gamma camera imaging, 10 µg IL-1 (0.68 mg/ml) was labelled with 222 MBq $Na^{123}I$ (Cygne, Eindhoven, The Netherlands, specific activity of $\geq2\times10^{17}$ Bq/mol) as described above.

The radiochemical purity of the radiopharmaceuticals was determined by instant thin-layer chromatography (ITLC) on Gelman ITLC-SG strips (Gelman Laboratories, Ann Arbor, Mich.) with 0.1 *M* citrate, pH 5.0, as the solvent.

Receptor binding assays

The murine cell line EL-4-6.1, a variant subline of EL-4 thymoma cells [9] and a kind gift from Dr. H.R. MacDonald (Ludwig Institute for Cancer Research Epalinges, Switzerland), was used for determination of the receptor binding capacity of the radioiodinated IL-1 preparations in vitro [10]. The cell line was cultured at 37°C in a humidified atmosphere of air/CO_2 (95:5) in RPMI 1640 medium (GIBCO, Gaithersburg, Md.) containing 10% fetal calf serum.

EL-4 binding assay. Live EL-4-6.1 cells were washed once with cold medium. A series of serially diluted cell suspensions ($0.2–3\times10^7$ cells/ml) was incubated with 10|000 cpm of radioiodinated IL-1 in assay buffer (RPMI 1640, 5 m*M* $MgCl_2$, 25 m*M* HEPES, 0.5% BSA, 20 µg/ml bacitracin (Sigma, St. Louis, Mo.). A duplicate of the lowest cell concentration was incubated in the presence of at least a 100-fold molar excess of unlabelled IL-1 to correct for non-specific binding. After 4 h incubation at 4°C, cells were centrifuged (5 min, 2000 *g*) and the radioactivity in the pellet (total bound radioactivity) was measured in a shielded well-type gamma counter (Wizard, Pharmacia-LKB, Sweden). The data were graphically analysed in a modified Lineweaver-Burk plot: a double inverse plot derived from the conventional binding plot (specifically bound activity versus cell concentration) [11]. The specific binding was obtained by subtracting the non-specific binding from the total bound radioactivity. The receptor binding fraction for conditions representing infinite cell receptor excess was calculated by linear extrapolation to the ordinate.

Scatchard analysis. The affinity of the IL-1R on EL-4-6.1 cells for radiolabelled IL-1 and the number of binding sites per cell were determined by means of a Scatchard analysis [12]. Briefly, live EL-4-6.1 cells were washed once with cold medium and incubated with serially diluted (1–1000 pmol/l) ^{125}I-IL-1. Non-specific binding was determined by incubating the EL-4-6.1 cells with labelled IL-1 in the presence of at least 100-fold excess of unlabelled IL-1. After 4 h of incubation at 4°C, cell-bound radioactivity was separated from unbound ^{125}I-IL-1 by centrifugation (5 min, 2000 *g*) and measured in the gamma counter.

Biodistribution experiments

As described previously, abscesses were induced in the left calf muscles of ether-anaesthetized female Swiss mice (20–25 g) with 2×10^7 colony forming units of *Staphylococcus aureus* in 0.05 ml 50%–50% suspension of autologous blood and normal saline [13]. Twenty-four hours after the inoculation of *S. aureus* in the muscle, when swelling of the muscle was apparent, a 0.2 ml mixture, containing 120 ng 0.4 MBq ^{125}I-IL-1 and 120 ng 0.4 MBq ^{131}I-myoglobin, was injected in the tail vein.

Groups of five mice were killed under ether anaesthesia by cervical dislocation at 2, 6, 12, 24 and 48 h after injection of the radiopharmaceuticals. Blood samples, infected left calf muscle, right calf muscle, thymus, lungs, spleen, kidneys, liver and intestines were collected. The dissected tissues were weighed and counted in the gamma counter. To correct for radioactive decay, injection standards were counted simultaneously. The measured activity in tissues and samples was expressed as percentage of injected dose per gram tissue (%ID/g). Abscess-to-contralateral muscle ratios and abscess-to-blood ratios were calculated.

Gamma camera imaging

Twenty-four hours after the induction of similar *S. aureus* infections, three Swiss mice were intravenously injected with 2 µg 18.5 MBq ^{123}I-IL-1. Potassium iodide was added to the drinking water to a final concentration of 1% to prevent uptake of free iodine in the thyroid. At 6, 24 and 48 h p.i., the mice were anaesthe-

tized with fluothane (ICI Farma, Rotterdam, The Netherlands) and placed prone on the gamma camera. The images were recorded with a standard large field of view gamma camera (Siemens Orbiter, Siemens Inc., Hoffmann Estate, Ill.) equipped with a parallel-hole medium-energy collimator. Images were obtained with a symmetrical 15% window over the 159-keV ^{123}I energy peak. After a minimum of 150|000 acquired counts, the images were digitally stored in a 256×256 matrix.

The scintigraphic results were analysed by drawing regions of interest over the abscess, the contralateral calf muscle (background) and the whole body. Abscess-to-background ratios and percentage residual activity in the abscess (abscess-to-whole body ratio ×100%) were calculated.

Statistical analysis

All values are expressed as mean ± standard error of the mean (SEM). Statistical analysis was performed using the repeated measures one-way analysis of variance (ANOVA).

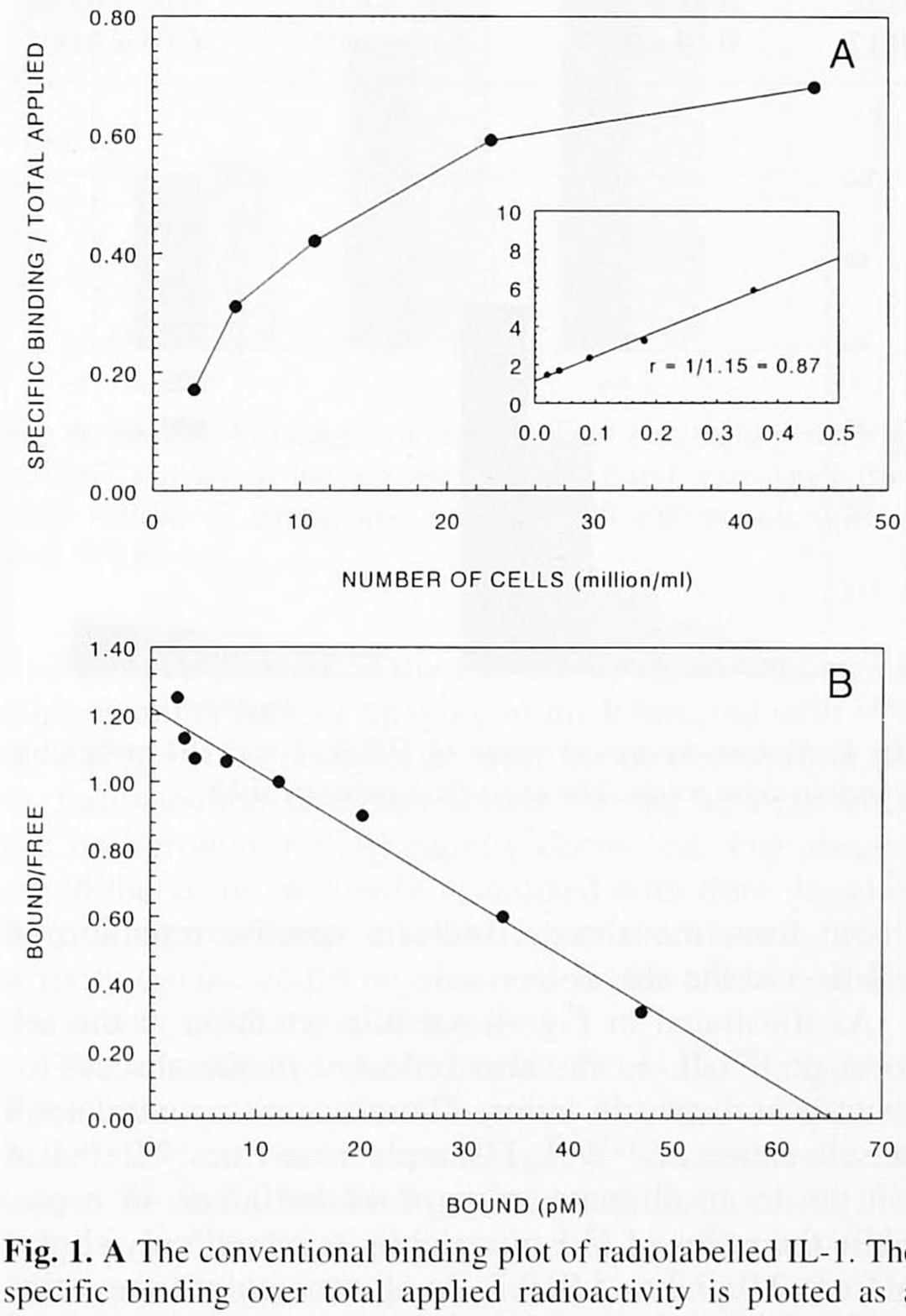

Fig. 1. A The conventional binding plot of radiolabelled IL-1. The specific binding over total applied radioactivity is plotted as a function of increasing cell concentration. The double inverse plot of radiolabelled IL-1 is shown in the *inset*. The receptor binding fraction for conditions representing infinite receptor excess (r) was calculated by linear extrapolation to the ordinate ($1/r$). **B** Scatchard analysis of radiolabelled IL-1 binding to EL-4-6.1 cells

Results

Receptor binding assays

The labelling efficiency was always between 50% and 80%. IL-1 was labelled with both Na^{125}I and Na^{123}I at a specific activity of 8–10 MBq/μg, indicating the average incorporation of one to two ^{125}I or ^{123}I atoms per IL-1 molecule. Similarly, myoglobin was labelled with ^{131}I at a specific activity of 7–8 MBq/μg. The radiochemical purity of all radiopharmaceuticals was higher than 98% after removal of unbound iodine.

The results of the EL-4 binding assay for radiolabelled IL-1 are shown in Fig. 1A. The non-specific binding was typically less than 5%. The calculated receptor binding fraction of radiolabelled IL-1 for conditions representing infinite cell receptor excess was always between 70% and 95%.

Scatchard analysis of the binding data of ^{125}I-IL-1 (Fig. 1B) revealed a dissociation constant of 5.4×10^{-11} mol/l. According to this analysis the EL-4-6.1 cells displayed 4400–8500 IL-1R per cell. In addition, the binding of ^{125}I-IL-1 to EL-4-6.1 cells could be completely inhibited by an excess of unlabelled IL-1 (IC_{50} value: 7.1×10^{-10} mol/l).

Biodistribution experiments and gamma camera imaging

Table 1 and Fig. 2 summarize the tissue biodistribution of radioiodinated IL-1 and myoglobin in mice with *S. aureus* infections. ^{125}I-IL-1 rapidly cleared from the blood. Two hours p.i., only 2.7% ID/g remained in the blood, while 12 h p.i. levels had decreased to less than 0.5% ID/g. Although the majority of peripheral blood cells are IL-1R positive cells, separate counting of plasma and cell pellet revealed that virtually all (>95%) of the label was found in the plasma fraction, apparently not cell bound. In addition, the plasma/cell pellet ratios for the ^{125}I label was not significantly different from those for the ^{131}I label at all time points, indicating that no significant specific binding to blood cells could be demonstrated. The absolute uptake of ^{125}I-IL-1 rapidly cleared from most organs to less than 1% ID/g at 12 h p.i. Most interestingly, from 12 h onwards the abscess is the organ with the highest activity.

The control agent, ^{131}I-myoglobin, cleared more slowly from the blood and hence from most organs, especially the kidneys. Most strikingly, despite the higher levels in the blood at all time points, no retention in the abscess could be observed. As shown in Fig. 3, ^{131}I-myoglobin cleared from the abscess during the time course of the experiment. In contrast, the abscess uptake of ^{125}I-IL-1 decreased at early time points but stabilized at approximately 1% ID/g from 12 h onwards. The abscess uptake of ^{131}I-myoglobin was significantly lower than that of ^{125}I-IL-1 from 12 h onwards ($P<0.05$). Abscess retention of ^{125}I-IL-1 and clearance of ^{131}I-myo-

Table 1. Biodistribution of ^{125}I-IL-1 and ^{131}I-myoglobin (%dose/g, mean values±SEM)

Organ	Radiopharmaceutical	2 h p.i.	6 h p.i.	12 h p.i.	24 h p.i.	48 h p.i.
Blood	^{125}I-IL-1	2.70 ± 0.34	1.57 ± 0.24	0.38 ± 0.20	0.08 ± 0.01	0.03 ± 0.004
	^{131}I-Myoglobin	5.09 ± 0.38	2.76 ± 0.12	1.22 ± 0.16	0.50 ± 0.02	0.17 ± 0.004
Abscess	^{125}I-IL-1	2.54 ± 0.24	1.64 ± 0.09	0.96 ± 0.18	0.81 ± 0.15	0.76 ± 0.11
	^{131}I-Myoglobin	2.40 ± 0.24	1.52 ± 0.04	0.74 ± 0.16	0.30 ± 0.03	0.15 ± 0.01
Muscle	^{125}I-IL-1	0.66 ± 0.05	0.34 ± 0.04	0.11 ± 0.04	0.03 ± 0.004	0.02 ± 0.002
	^{131}I-Myoglobin	1.20 ± 0.17	0.67 ± 0.13	0.21 ± 0.09	0.06 ± 0.002	0.03 ± 0.002
Thymus	^{125}I-IL-1	1.73 ± 0.24	0.81 ± 0.11	0.30 ± 0.12	0.24 ± 0.11	0.04 ± 0.004
	^{131}I-Myoglobin	1.59 ± 0.26	0.79 ± 0.10	0.37 ± 0.13	0.21 ± 0.06	0.07 ± 0.01
Lung	^{125}I-IL-1	4.31 ± 0.45	1.54 ± 0.23	0.41 ± 0.17	0.12 ± 0.02	0.03 ± 0.004
	^{131}I-Myoglobin	2.89 ± 0.23	1.63 ± 0.11	0.75 ± 0.16	0.32 ± 0.02	0.11 ± 0.009
Spleen	^{125}I-IL-1	5.36 ± 0.60	1.81 ± 0.18	0.50 ± 0.10	0.17 ± 0.04	0.04 ± 0.004
	^{131}I-Myoglobin	2.45 ± 0.20	1.45 ± 0.12	0.72 ± 0.11	0.36 ± 0.04	0.24 ± 0.009
Kidney	^{125}I-IL-1	4.84 ± 0.33	1.47 ± 0.13	0.51 ± 0.16	0.21 ± 0.01	0.10 ± 0.009
	^{131}I-Myoglobin	8.72 ± 0.25	4.34 ± 0.13	2.35 ± 0.22	1.53 ± 0.04	0.92 ± 0.07
Liver	^{125}I-IL-1	3.12 ± 0.27	0.86 ± 0.10	0.28 ± 0.08	0.10 ± 0.009	0.05 ± 0.004
	^{131}I-Myoglobin	3.01 ± 0.20	1.82 ± 0.11	1.09 ± 0.11	0.71 ± 0.02	0.46 ± 0.01
Intestine	^{125}I-IL-1	2.59 ± 0.35	1.55 ± 0.22	0.48 ± 0.22	0.11 ± 0.02	0.03 ± 0.004
	^{131}I-Myoglobin	2.18 ± 0.33	1.23 ± 0.17	0.49 ± 0.19	0.15 ± 0.02	0.05 ± 0.002

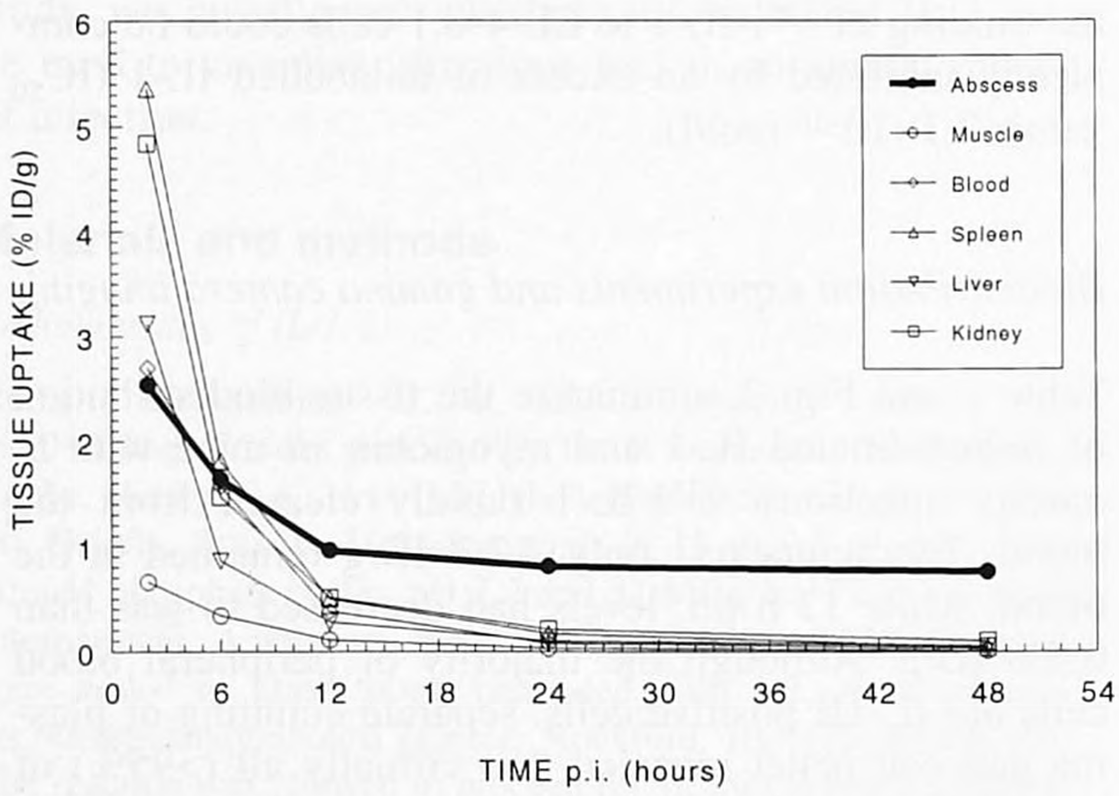

Fig. 2. Tissue uptake of ^{125}I-IL-1 in several organs at various time points, expressed as %dose/g. The corresponding SEM are reported in Table 1

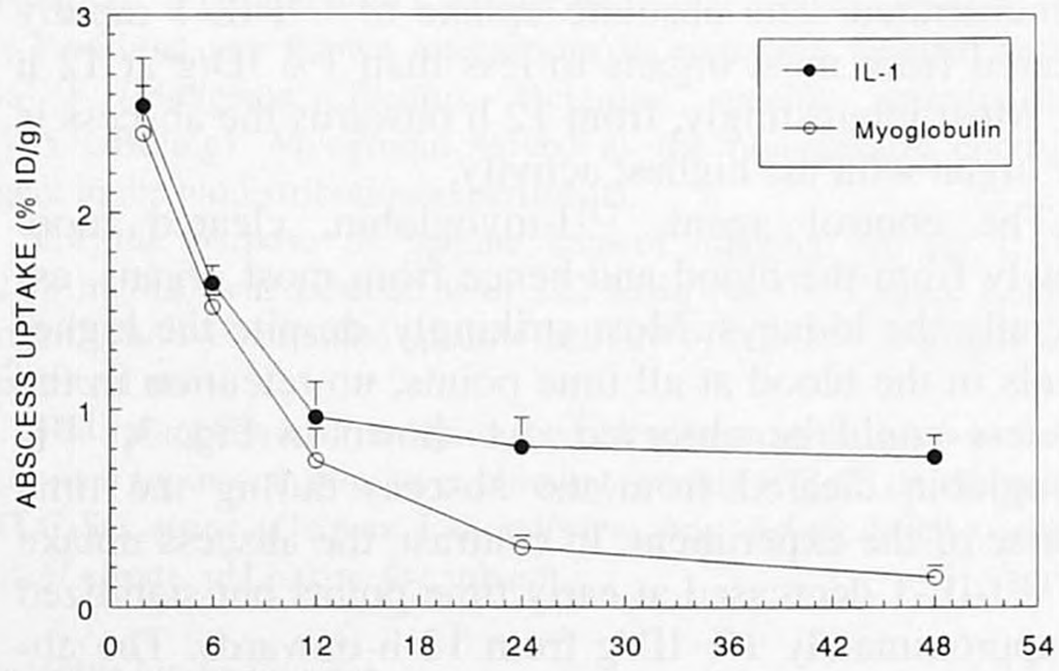

Fig. 3. The absolute abscess uptake of ^{125}I-IL-1 and ^{131}I-myoglobin at various time points, expressed as %dose/g. The *error bars* indicate SEM

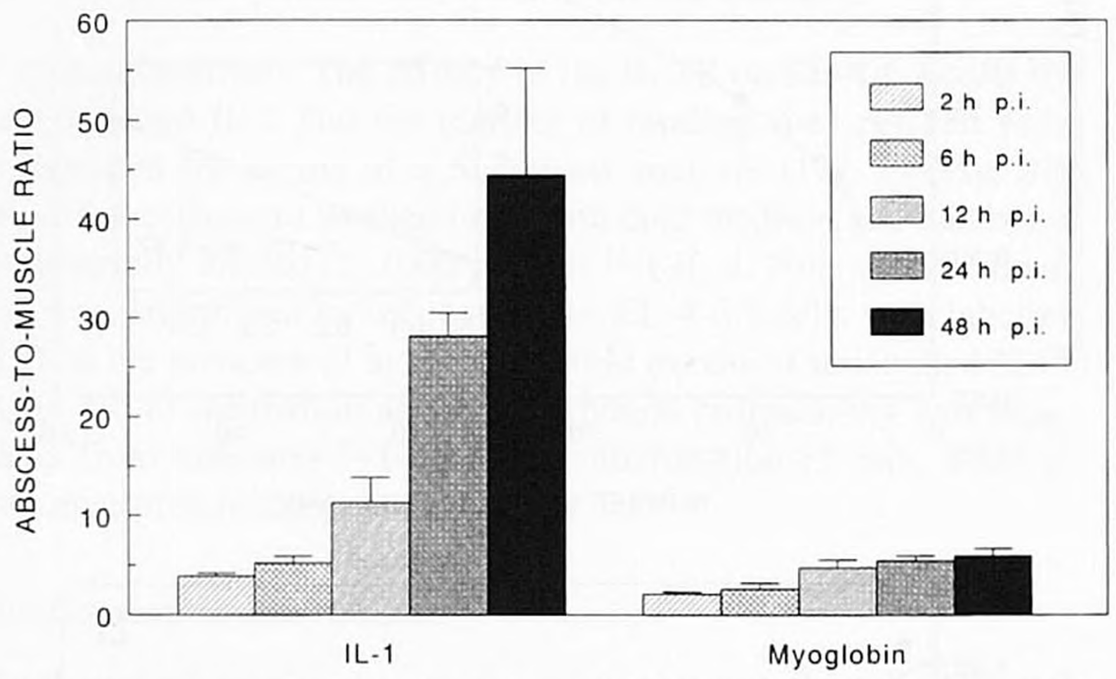

Fig. 4. Abscess-to-muscle ratios of ^{125}I-IL-1 and ^{131}I-myoglobin at various time points. The *error bars* indicate SEM

globin from the abscess indicate specific retention of ^{125}I-IL-1 in the abscess.

As illustrated in Fig. 4, specific retention in the abscess of ^{125}I-IL-1 was also reflected in the abscess-to-contralateral muscle ratios. The abscess-to-contralateral muscle ratios of ^{125}I-IL-1 sharply rose from 3.9±0.3 at 2 h p.i. to an ultimate value of 44.4±10.8 at 48 h p.i., while the ratios of ^{131}I-myoglobin increased only slightly from 2.0±0.2 to 5.9±0.7. At all time points, the ratios of ^{125}I-IL-1 were significantly higher than the ratios of the control agent ($P<0.05$). Comparison of the abscess-to-blood ratios of both agents demonstrated that the retention of ^{125}I-IL-1 in the abscess was not just caused by increased perfusion to the site of infection: the continuously increasing abscess-to-blood ratios of ^{125}I-IL-1 from 1.0±0.2 at 2 h p.i. to 28.4±5.1 at 48 h p.i. were at all time points significantly higher than the corresponding ratios of ^{131}I-myoglobin, which did not exceed the value of 0.9±0.08 ($P<0.04$).

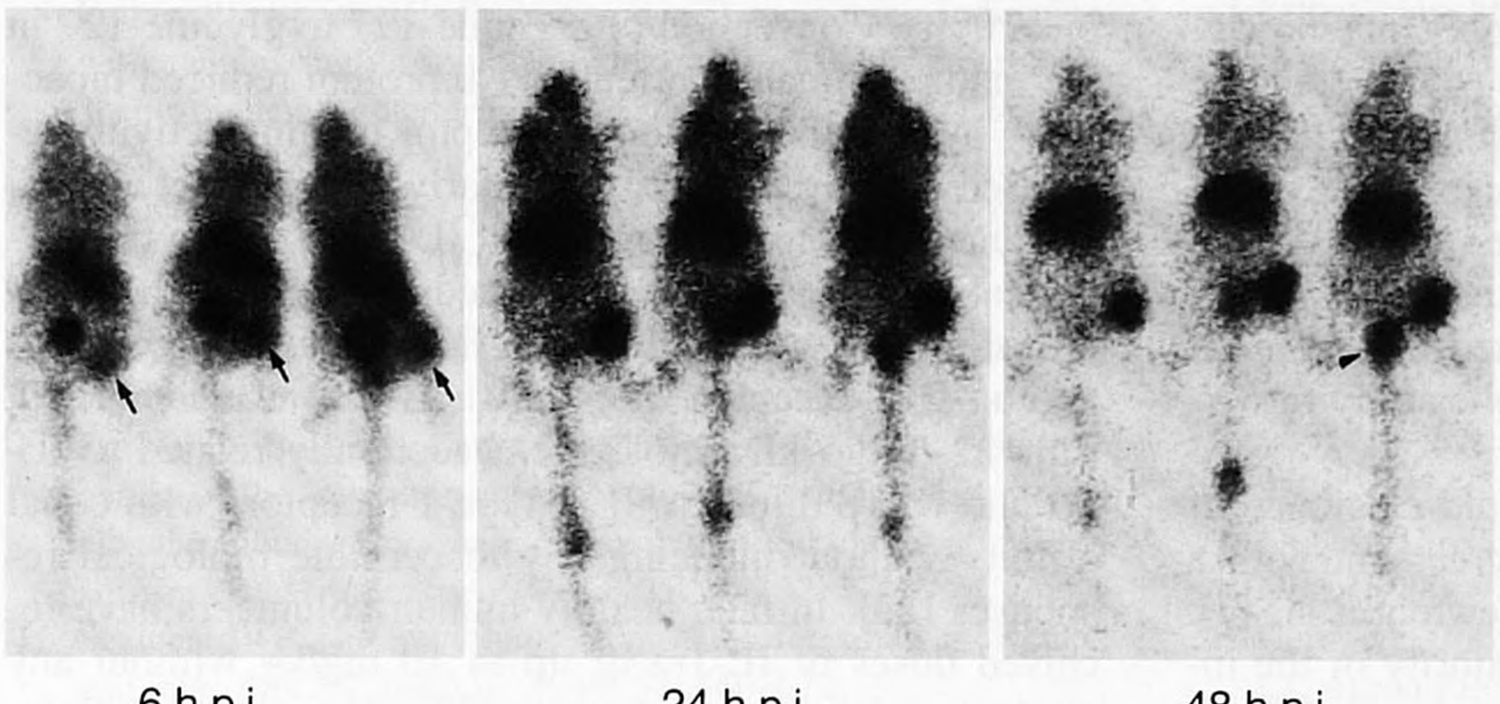

Fig. 5. Images of mice with an *S. aureus* infection in the left calf muscle, injected with ^{123}I-IL-1, at 6, 24 and 48 h p.i. The abscesses are indicated by the *arrows*. The retention of ^{123}I-IL-1 in the abscess became more prominent over a 48-h time span. At 48 h p.i. the mouse on the right showed activity at the base of the tail due to urinary contamination (*arrowhead*)

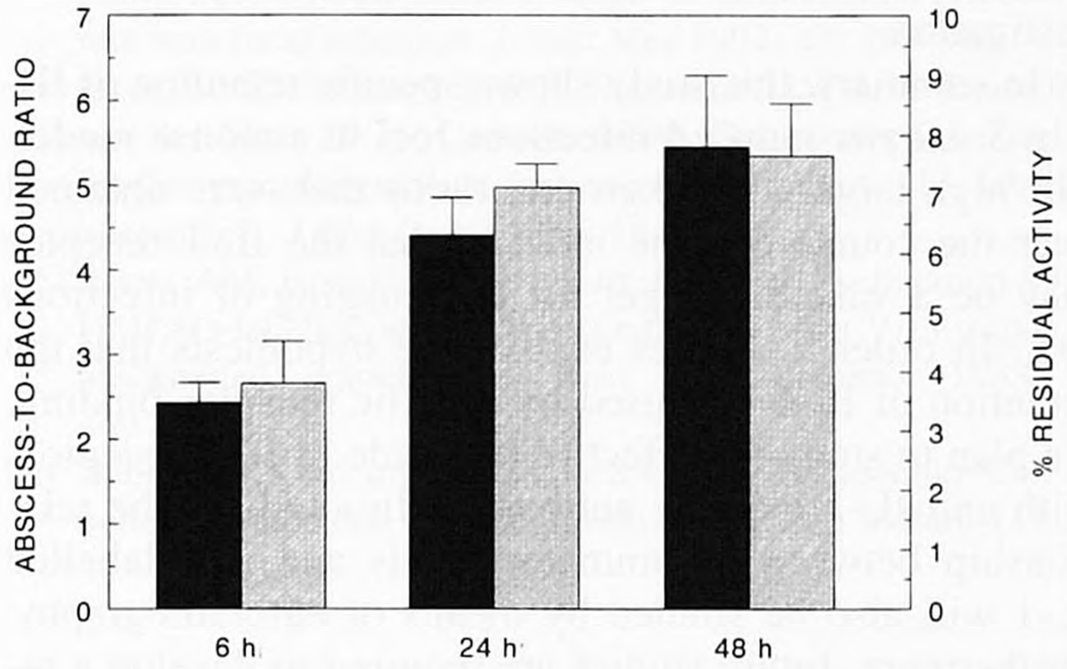

Fig. 6. Abscess-to-background ratios (*solid bars*) and percentage residual activity in the abscess (*hatched bars*), calculated from mice with an *S. aureus* abscess in the left calf muscle injected with ^{123}I-IL-1

The accumulation in the abscess was also demonstrated by gamma camera imaging of mice injected with ^{123}I-IL-1 (Fig. 5). In accordance with the biodistribution data, radiolabelled IL-1 was retained in the abscess while the background activity rapidly decreased. The abscess could therefore be clearly visualized with time. In addition to accumulation of ^{123}I-IL-1 in the abscess, some activity uptake could be observed in the bladder and in the stomach (≤0.1% at 48 h p.i.).

The quantitative data derived from the images of three mice confirmed the observed retention of radiolabelled IL-1 in the abscess (Fig. 6). A continuous increase in abscess-to-background ratio from 2.4±0.1 at 6 h p.i. to 5.5±0.6 at 48 h p.i. could be observed. Furthermore, the percentage of residual activity in the abscess increased as well and reached the value of 7.6%±0.6% at 48 h p.i.

Discussion

In this study, we investigated IL-1 as a vehicle to image infectious foci. Both the biodistribution and the imaging studies showed that radioiodinated IL-1 was retained in the infectious focus. The retention was specific since the abscess uptake of IL-1 remained high as compared to the size-matched control agent myoglobin in spite of the slower clearance of myoglobin from most other tissues. Forty-eight hours p.i. the abscess-to-muscle ratio for IL-1 was more than 7 times higher than the ratio obtained with myoglobin (44.4±10.8 (vs) 5.9±0.7). This supports the hypothesis that IL-1 is retained at the infectious site because of interaction with its receptor on inflammatory cells.

The in vitro binding data demonstrated that IL-1 was still able to bind its receptor after the radiolabelling procedure. Several radioiodination methods, i.e. the glucose-oxidase/lactoperoxidase method, the Bolton-Hunter method and the iodogen method, had been compared for the in vitro receptor binding of radiolabelled IL-1 and the labelling efficiency. The iodogen method yielded the best results and was therefore selected. To demonstrate specific receptor binding of radiolabelled IL-1 in vivo in the abscess, we carefully searched for the proper control agent in the biodistribution studies. Ideally, this agent should have an identical molecular structure to IL-1, but lack the receptor binding capacity. In order to obtain such a control agent, we performed experiments in which efforts were made to heat-inactivate IL-1. The heat (≥60°C) abolished the receptor binding capacity. However, size exclusion of heat-inactivated IL-1 on a Sephadex G75 column (Pharmacia Fine Chemicals, Uppsala, Sweden) showed that the heat caused protein aggregation. A non-denaturated size-matched protein without any known interactions with the IL-1R in vivo appeared to be the best possible alternative. Myoglobin met these requirements. Unfortunately, the clearance from the blood and most other tissues was somewhat slower than the clearance of radiolabelled IL-1. Most strikingly, however, the clearance from the abscess was much faster than the clearance of radiolabelled IL-1, supporting the concept of specific binding of IL-1 to the inflammatory cells in the infectious focus. Two binding mechanisms could theoretically play a role: (a) IL-1 binds to IL-1 receptor positive cells in the infectious focus, and (b) IL-1 binds to these cells in the blood compartment followed by transport to the site of infection. Our results suggest that the interaction with the IL-1 re-

ceptor takes place at the focus of infection, since no significant binding to peripheral blood cells (<5%) could be demonstrated. A specific receptor binding mechanism may imply a greater specificity for the imaging of inflammation and infection than is obtained with ^{111}In-labelled human polyclonal IgG, which we currently favour for clinical use. We recently demonstrated that ^{111}In-labelled IgG is taken up at inflammatory sites only by virtue of vascular leakage [13, 14].

Our pharmacokinetic data showed rapid clearance of ^{125}I-IL-1 from the body, which is in agreement with a study in uninfected mice reported by Newton et al. [7]. These authors found excretion of the majority of the injected dose via the kidneys within the first hours following injection. In their study, almost all the radioactivity found in the urine was associated with intact 17-kDa IL-1. Accumulation in the kidney was not observed in our study, indicating that radiolabelled IL-1 was rapidly excreted in the urine, which is in line with the activity present in the bladder on our images.

The abscess-to-contralateral muscle ratio of ^{125}I-IL-1 of 44.4±10.8 at 48 h p.i. in our biodistribution study was clearly higher than the ratios obtained with other infection detection agents, such as ^{111}In-labelled human polyclonal IgG and ^{99m}Tc-labelled leucocytes [13, 15]. Comparable ratios were obtained in recent studies with other radiopharmaceuticals: a study by Babich et al. reported a ratio of 33.6 after 18 h with ^{99m}Tc-labelled chemotactic peptides in rabbits [16], while in another study in rats a ratio of 35.3 was found after 24 h using ^{99m}Tc-labelled liposomes [17]. The background activity of ^{125}I-IL-1 cleared much faster than both radiolabelled chemotactic peptides and liposomes. In our study, the abscess was the organ with the highest activity after 12 h, while both ^{99m}Tc-labelled chemotactic peptides and liposomes show high uptake in the mononuclear phagocytic system [18], as can also be seen on the images obtained with these agents. The fast whole body clearance and the retention in the abscess of ^{123}I-IL-1 resulted in clearly delineated abscesses. The modest uptake in the stomach on our images is due to a certain degree of dehalogenation, as is generally recognized for radioiodinated proteins.

The rapid clearance resulted in a low absolute uptake of radiolabelled IL-1 in the abscess. Therefore, to apply radiolabelled IL-1 clinically for scintigraphic visualization of infectious foci, high doses of radioactivity and subsequently high doses of IL-1 would have to be administered. The latter will interfere with clinical application because of the side-effects of systemically administered IL-1. Fever, headache, increased sensitivity to pain and hypotension are commonly seen when IL-1 is administered to patients even at doses as low as 10–100 ng/kg [19]. Obviously, these are unacceptable side-effects for an imaging agent. They might be circumvented by using a molecule that binds to the IL-1R with the same affinity, without inducing biological reponses. Site-directed mutagenesis has elucidated particular amino acid residues in the IL-1 molecule which affect the bioactivity. Conversion of arginine-127 to glycine-127 in the mature human interleukin-1 b protein reduced bioactivity by 100-fold while the receptor binding activity decreased by only 25% [20]. Similarly, Camacho et al. [21] produced the Thr9Gly mutant of IL-1β of which the biological activity had been reduced 200-fold without diminishing the receptor binding. Furthermore, a few years ago an IL-1 receptor antagonist (IL-1ra) was identified. This 22- to 25-kDa molecule, structurally related to IL-1α and IL-1β, binds to IL-1 type 1 receptors with equal affinity without inducing any discernible biological responses [22]. In fact, healthy human volunteers have received doses of IL-1ra of up to 10 mg/kg without any clinical or laboratory changes [23]. The use of radiolabelled IL-1ra in our animal model is currently under investigation.

In summary, this study shows specific retention of IL-1 in *S. aureus*-induced infectious foci in a mouse model. The high target-to-background ratios that were obtained over the course of time indicate that the IL-1 receptor may be a valuable target for the imaging of infectious foci. In order to further explore the hypothesis that the retention of IL-1 is caused by specific receptor binding, we plan to study the effect of blockade of IL-1 receptors with anti-IL-1 receptor antibodies. In addition, the relationship between inflammatory cells and radiolabelled IL-1 will also be studied by means of autoradiography. Furthermore, future studies are required to develop a radiopharmaceutical directed towards the same target but lacking the clinical side-effects of IL-1.

Acknowledgements. The authors thank Mr. H.J.J. van Lier, PhD (University of Nijmegen, Department of Medical Statistics) for his advice in performing the statistical analysis, Mr. A. Ross, PhD (University of Nijmegen, Department of Endocrinology) for his assistance in performing the Scatchard analysis and Mr. G. Grutters and Mr. H. Eijkholt (University of Nijmegen, Central Animal Laboratory) for technical assistance.

References

1. Corstens FHM, Oyen WJG, Becker WS. Radioimmunoconjugates in the detection of infection and inflammation. *Semin Nucl Med* 1993; 23: 148–164.
2. Corstens FHM, van der Meer JWM. Chemotactic peptides: new locomotion for imaging of infection? *J Nucl Med* 1991; 32: 491–494.
3. Signore A, Chianelli M, Toscano A, et al. A radiopharmaceutical for imaging areas of lymphocytic infiltration: ^{123}I-interleukin-2. Labelling procedure and animal studies. *Nucl Med Commun* 1992; 13: 713–722.
4. Hay RV, Skinner RS, Newman OC, et al. Nuclear imaging of acute inflammatory lesions with recombinant human interleukin-8 [abstract]. *J Nucl Med* 1993; 34: 104P.
5. Dinarello CA. Interleukin-1 and interleukin-1 antagonism. *Blood* 1991; 77: 1627–1652.
6. Ward PA. Chemotaxis. In: Parker CW, ed. *Clinical immunology, 1st edn*. Philadelphia: W.B. Saunders; 1980: 272–297.
7. Newton RC, Uhl J, Covington M, Back O. The biodistribution and clearance of radiolabelled human interleukin-1 beta in mice. *Lymphokine Res* 1988; 7: 207–210.

8. Fraker PJ, Speck JC. Protein and cell membrane iodination with a sparingly soluble chloramide 1,3,4,6-tetrachloro-3α,6α-diphenyl-glucouril. *Biochem Biophys Res Commun* 1978; 80: 849–857.
9. Zubler RH, Erard F, Lees RK, et al. Mutant EL-4 thymoma cells polyclonally activate murine and human B cells via direct cell interaction. *J Immunol* 1985; 134: 3662.
10. Lowenthal JW, MacDonald HR. Binding and internalization of interleukin-1 by T-cells. *J Exp Med* 1986; 164: 1060–1074.
11. Lindmo T, Boven E, Cuttitta F, Fedorko J, Bunn PA. Determination of the immunoreactive fraction of radiolabelled monoclonal antibodies by linear extrapolation to binding at infinite antigen excess. *J Immunol Methods* 1984; 72: 77–89.
12. Scatchard G. The attractions of proteins for small molecules and ions. *Ann NY Acad Sci* 1949; 51: 660–672.
13. Oyen WJG, Claessens RAMJ, van der Meer JWM, Corstens FHM. Biodistribution and kinetics of radiolabelled proteins in rats with focal infection. *J Nucl Med* 1992; 33: 388–393.
14. Oyen WJG, Claessens RAMJ, Raemakers JMM, de Pauw BE, van der Meer JWM, Corstens FHM. Diagnosing infection in febrile granulocytopenic patients with indium-111 labelled human IgG. *J Clin Oncol* 1992; 10: 61–68.
15. Peters AM, Roddie ME, Danpure HJ, et al. Technetium-99m-HMPAO-labelled leucocytes: comparison with ^{111}In-tropolonate-labelled granulocytes. *Nucl Med Commun* 1988; 9: 449–463.
16. Babich JW, Graham W, Barrow SA, et al. Technetium-99m-labelled chemotactic peptides: comparison with indium-111-labelled white blood cells for localizing acute bacterial infection in the rabbit. *J Nucl Med* 1993; 34: 2176–2181.
17. Goins B, Klipper R, Rudolph AS, Cliff RO, Blumhardt R, Phillips WT. Biodistribution and imaging studies of technetium-99m-labelled liposomes in rats with focal infection. *J Nucl Med* 1993; 34: 2160–2168.
18. Van Furth R, Cohn ZA, Hirsch JG, et al. The mononuclear phagocytic system: a new classification of macrophages, monocytes, and their precursor cells. *Bull World Health Organ* 1972; 46: 845–852.
19. Smith J, Urba W, Steis R, et al. Interleukin-1 alpha: results of a phase I toxicity and immunomodulatory trial. *Am Soc Clin Oncol* 1990; 9: 717.
20. Gehrke L, Jobling SA, Paik LSK, McDonald B, Rosenwasser LJ, Auron PE. A point mutation uncouples human interleukin-1β biological activity and receptor binding. *J Biol Chem* 1990; 265: 5922–5925.
21. Camacho NP, Smith DR, Goldman A. Structure of an interleukin-1β mutant with reduced bioactivity shows multiple subtle changes in conformation that affect protein-protein recognition. *Biochemistry* 1993; 32: 8749–8757.
22. Arend WP. Interleukin 1 receptor antagonist. A new member of the interleukin 1 family. *J Clin Invest* 1991; 88: 1445–1451.
23. Granowitz EV, Porat R, Mier JW, et al. Pharmacokinetics, safety and immunomodulatory effects of human recombinant interleukin-1 receptor antagonist in healthy humans. *Cytokine* 1992; 4: 353–360.